THE JOURNAL OF PHYSICAL CHEMISTRY B

Article

pubs.acs.org/JPCB

Excited-State Proton Transfer in Confined Medium. 4-Methyl-7-hydroxyflavylium and β-Naphthol Incorporated in Cucurbit[7]uril

Nuno Basílio,* César A. T. Laia, and Fernando Pina*

REQUIMTE, Departamento de Química, Faculdade de Ciências e Tecnologia, Universidade Nova de Lisboa, 2829-516 Monte de Caparica, Portugal

ABSTRACT: Excited-state proton transfer (ESPT) was studied by fluorescent emission using a mathematical model recast from the Weller theory. The titration curves can be fitted with three parameters: pK_a (acidity constant of the ground sate), pK^*_{ap} (apparent acidity constant of the excited state), and η_{A^*}, the efficiency of excited base formation from the excited acid. β-Naphthol and 4-metyhl-7-hydroxyflavylium were studied in aqueous solution and upon incorporation in cucurbit[7]uril. For all the compounds studied the interaction with the host leads to 1:1 adducts and the ground-state pK_a increases upon incorporation. Whereas the ESPT of 4-methyl-7-hydroxyflavylium practically does not change in the presence of the host, in the case of β-naphthol it is prevented and the fluorescence emission titration curves are coincident with those taken by absorption. The position of the guest inside the host was investigated by NMR experiments and seems to determine the efficiency of the ESPT. The ESPT decreases for the guest, exhibiting a great protection of the phenol to the bulk water interaction.

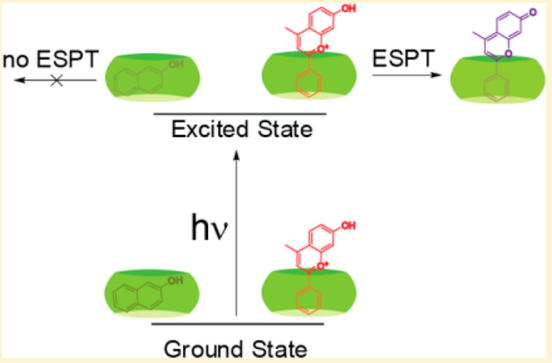

INTRODUCTION

Excited-state proton transfer together with excited-state electron transfer are two of the most studied reactions in chemistry from both experimental and theoretical points of view.[1−7] The cascade of events that follow the light absorption,[2] leading to the proton transfer, can be analyzed by the simplified Scheme 1. The excited-state rate constants reported in Scheme 1 should be viewed as a function of other constants regarding the sequence of events (e.g., solvated pair formation and dissociation are included in k^*_a), i.e., they are global constants observed in the time scale of pico- to nanoseconds. In spite of not giving the mechanistic details of the proton transfer, Scheme 1 is very adequate to account for the steady-state fluorescence emission titrations and to obtain relevant information in particular when different compounds are compared. It should be stressed that a detailed analysis of the ultrafast kinetic processes is beyond the scope of this work.

Scheme 1. Excited-State Proton Transfer Equilibrium under Steady-State Irradiation

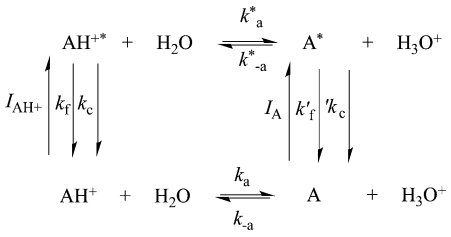

Steady-state fluorescence emission and the respective theory were reported by Weller,[8,9] Selinger,[10,11] and Shizuka.[6] In Scheme 1, the sequence of chemical reactions taking place under steady-state irradiation is presented.[12,13]

In Scheme 1, I_{AH+} and I_A are the light absorbed by the acid and base, respectively; k_f and k'_f the fluorescence emission constants for the acid and base, respectively; and k_c and k'_c the sum of all the constants regarding the nonradiative processes for the acid and base, respectively.

Some years ago we recast the Weller model in terms of three macroscopic parameters: two sigmoid curves for the ground and excited state (accounted for the respective pK_a) and an efficiency, η_{A^*}, see below.[12,13] When buffer effects are neglected, which is experimentally achieved if the buffer concentration is maintained small (typically, at 0.01 M no significant effect is observed[12]), the following mathematical expressions account for the process if excitation at the isosbestic point of the acid and base ground-state absorption is used[12,13]

$$\frac{\phi}{\phi_0} = \alpha\alpha'^* + \beta\alpha^* \quad (1)$$

$$\frac{\phi'}{\phi'_0} = \alpha\beta'^* + \beta\beta^* \quad (2)$$

Special Issue: Photoinduced Proton Transfer in Chemistry and Biology Symposium

Received: November 12, 2014
Revised: November 14, 2014

   dx.doi.org/10.1021/jp511351w | J. Phys. Chem. B XXXX, XXX, XXX−XXX

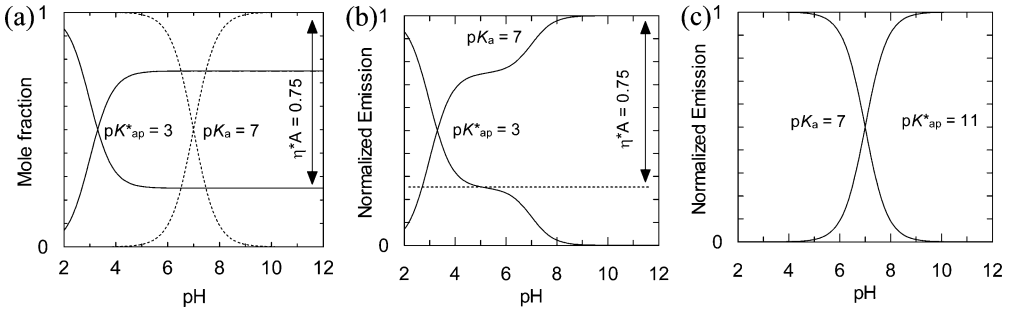

Figure 1. (a) Simulation of the mole fraction distribution of the acid and base species (α and β respectively) in the ground state (full line) and the functions α'^* and β'^* of the excited state (dashed line) for $pK_a = 7$, $pK^*_{ap} = 3$, and $\eta_{A^*} = 0.75$; (b) simulation of the fluorescence titration curve for the same parameters using eq 5; (c) same as in panel b for $pK_a = 7$ and $pK^*_{ap} = 11$ independent from the η_{A^*} value.

where ϕ and ϕ_0 are the fluorescence emission quantum yields at a certain pH value and at the maximum for the acid, and ϕ' and ϕ'_0 are the equivalent for the base. The ratio of the fluorescence emission intensities could be used because it is equal to that of the quantum yields, and the excitation wavelength should take place at the isosbestic point of the acid and base absorption spectra to avoid corrections for the absorbed light.

$$\alpha = \frac{[H^+]}{[H^+] + K_a}; \quad \beta = \frac{K_a}{[H^+] + K_a} \tag{3}$$

$$\alpha^* = \frac{[H^+]}{[H^+] + K^*_{ap}}; \quad \beta^* = \frac{K^*_{ap}}{[H^+] + K^*_{ap}} \tag{4}$$

$$\alpha'^* = 1 - \frac{\eta^*_A K^*_{ap}}{[H^+] + K^*_{ap}} = 1 - \eta^*_A \beta^*;$$

$$\beta'^* = \frac{\eta^*_A K^*_{ap}}{[H^+] + K^*_{ap}} = \eta^*_A \beta^* \tag{5}$$

$$K^*_{ap} = \frac{k^*_{ap}\tau_{AH^+}}{k^*_{-a}\tau_A}\frac{1}{\eta^*_A} \tag{6}$$

$$\eta^*_A = \frac{k^*_a}{k_f + k_c + k^*_a} \tag{7}$$

The titration curves of the ground state are dependent on the parameter pK_a, while the titration curves of the excited state are dependent on two parameters: pK^*_{ap} (the experimental pK of the excited sate) and the parameter η_{A^*} accounting for the efficiency of the base formation from the acid in the excited state. A very small value of η_{A^*} makes the fluorescence emission titration curves undistinguishable from those of absorption, and no information about the excited state is available. The same occurs when $pK_a > pK^*_a$.[12]

In Figure 1, the simulation of the shape of the mole fraction distribution as a function of pH for $pK_a = 7$ and the same for the "excited-state functions" for $pK^*_{ap} = 3$ and $\eta_{A^*} = 0.5$ are shown.

Figure 1 illustrates the general behavior of phenols fluorescence emission titration curves, where the pK_a of the ground state is generally higher than the one of the excited state. The emission from the acid shows a plateau between pH 4 and 6. At these pH values the only species present in the ground state and therefore absorbing light is the acidic form. The existence of the plateau is due to the lack of reversibility in the excited state because the formation of AH^{+*} from A* is negligible ($k^*_a[H^+] \ll k^*_a$ at these pH values). The decreasing of the fluorescence emission curve of the acid species from the plateau to zero occurs because the direct excitation of the acid decreases in the same way ($pK_a = 7$). The acidic plateau is accompanied by a symmetric plateau of the base as a consequence of the formation of A* from excitation of AH^+. The growing of the base emission at higher pH values results from its direct excitation. When the pK^*_{ap} is higher than pK_a, as the example in Figure 1c, the fluorescence emission titration curves are coincident with those obtained by titration of the absorption.

Synthetic and natural dyes belonging to the flavylium family of compounds display a rich and very interesting set of physicochemical properties in the ground and excited states. These molecules have been claimed as superphotoacids because they undergo ultrafast and highly efficient ESPT.[14] This phenomenon had been extensively investigated both in bulk solution and in micellar systems.[15,16] However, the ESPT of flavylium compounds in the confined space of molecular nanocavities has not been reported. This should be addressed because the physicochemical properties of molecules encapsulated in confined spaces can be dramatically different from those observed in bulk solution. In addition, their behavior in such restricted media can resemble that displayed in the pockets and inner spaces of large biochemical structures.[17] In this work the above-described theoretical procedure is used to characterize the ESPT of a representative molecule of this family (4-methyl-7-hydroxyflavylium) along with the iconic β-naphthol in water and upon incorporation in cucurbit[7]uril (CB7). Cucurbit[n]urils (n = 5−10) are pumpkin-shaped macrocyclic host molecules formed by glycoluril units linked by methylene bridges. Their hydrophobic cavity associated with the large negative electrostatic potential at the portals of the cavity, lined by the carbonyl oxygen atoms, make them excellent candidates to form inclusion complexes with organic cations.[18−20] In fact, it was previously demonstrated by some of us that CB7 forms stable inclusion complexes with a flavylium cation.[21]

EXPERIMENTAL SECTION

β-Naphthol and cobaltocenium hexafluorophosphate were purchased from commercial suppliers and used without further purification. 4-Methyl-7-hydroxyflavylium was available from previous works.[22,23] The synthesis of cucurbit[7]uril (CB7) was carried out according to a previously described procedure and characterized by ^{1}H NMR.[24] Stock solutions of CB7 were

dx.doi.org/10.1021/jp511351w | J. Phys. Chem. B XXXX, XXX, XXX−XXX

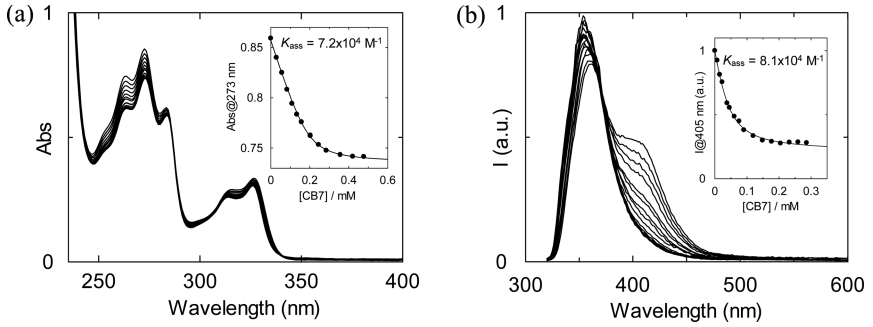

Figure 2. (a)Absorption and (b) fluorescence emission of β-naphthol as a function of CB7 concentration. All experiments were carried out at 21 °C. The fluorescence spectra were acquired with excitation at 310 nm. The concentration of β-naphthol was kept constant and equal to 0.19 mM and 0.039 mM in the absorption and fluorescence emission titration experiments, respectively. The insets show the variation of the absorbance or emission at a fixed wavelength as a function of CB7 concentration along with the fitting line for a 1:1 binding isotherm. The pH was carefully checked after each addition of CB7.

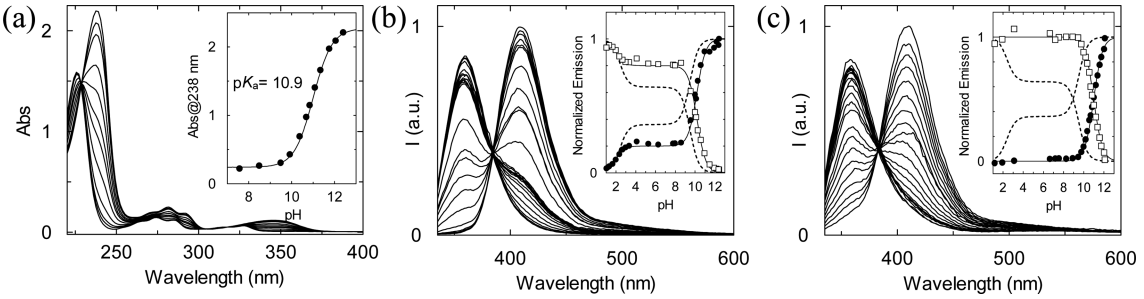

Figure 3. (a) pH-dependent absorption spectra of β-naphthol (4.2×10^{-2} mM) in the presence of 1 mM CB7. (b) pH-dependent emission spectra of β-naphthol (2.9×10^{-2} mM) in the presence of 0.125 mM CB7. (c) The same as in panel b in the presence of 1 mM CB7. The insets show (a) the absorbance changes observed at 238 nm as a function of the pH and (b, c) the corresponding normalized fluorescence emission from the acid species (open squares, 359 nm) and from the basic species (closed circles, 409 nm) along with the simulated curve (dashed line) in the absence of CB7 for comparison. Fitting was achieved by means of eqs 1 and 2: dashed line in the absence of CB7, pK_a = 9.5, pK^*_{ap} = 2.4, and η_{A^*} = 0.36 (taken from ref 13); in the presence of (b) cucurbit[7]uril (0.125 mM), pK_a = 10.2, pK^*_{ap} = 2.4, and η_{A^*} = 0.21 and (c) cucurbit[7]uril (1 mM), pK_a = 11.0, and η_{A^*} = 0.

titrated with cobaltocenium by ultraviolet−visible (UV−vis) absorption spectroscopy.[25] UV−vis absorbance spectra were acquired on a UV−vis−NIR Varian Cary 5000 spectrophotometer and fluorescence spectra were recorded on a SPEX Fluorolog-3 Model FL3−22 spectrofluorimeters. Flash photolysis experiments were run on a LKS.60 ns laser photolysis spectrometer from Applied Photophysics, with a Brilliant Q-Switch Nd:YAG laser from Quantel, using the second harmonic (λ_{exc} =355 nm, laser pulse half-width equal to 6 ns). The Glotaran software was employed for global analysis (at multiple wavelengths) of the flash photolysis time-resolved spectroscopic data.[26] During the fitting procedure a Gaussian instrument response function (IRF) was considered to take into account the convolution of the transient absorption signal with the laser pulse. The kinetic data was analyzed with three components: (a) The first component takes care of the luminescent contamination of the transient absorption data (fluorescence), giving negative pre-exponentials with the same shape of the emission spectra. (b) The second component is from the transient absorption spectra assigned to the ground-state proton recombination, which is the major component of the decay that is the subject of this communication. (c) Finally, a photochemical offset that accounts for some extra-photochemical reactions that eventually lead to photodegradation of the compound (this is a minor correction). NMR experiments were conducted on a Bruker AMX 400 spectrometer operating at 400.13 MHz (^{1}H) and 100.00 MHz (^{13}C). The pH of the solutions was measured on a pH-Meter BASIC 20+ (CRISON) and adjusted by addition of concentrated HCl or NaOH. For highly acidic solutions the pH was corrected by the Hammett's acidity function (H_0).[27]

RESULTS AND DISCUSSION

ESPT of β-Naphthol in the Presence of Cucurbit[7]uril.

The compound β-naphthol is an icon for the study of ESPT. It was "the molecule" used by Weller during the 1950s to illustrate his interpretation of fluorimetric titrations. Given the historical importance of this molecule, we have decided to selected it as a guest and study his pH-dependent emission properties in the presence of cucurbit[7]uril (CB7).

Figure 2 shows the variations observed in the absorption (Figure 2a) and emission (Figure 2b) spectra of β-naphthol upon the gradual addition of CB7 at pH 6.0 ± 0.2. Fitting the observed changes in the absorption spectra as a function of the CB7 concentration to a 1:1 binding isotherm allows the determination of an association constant of $(7.2 \pm 2.0) \times 10^4$ M^{-1}. Figure 2b shows the fluorescence emission spectra of β-naphthol as a function of the CB7 concentration at pH 6.0 ± 0.2. In the absence of host, the emission spectra is composed by two bands: one assigned to emission of the acid form, and the other, red-shifted, assigned to the anionic base. Inspection of the emission curves as a function of the CB7 concentration indicates that the emission from the anionic species decreases by increasing the CB7 concentration. The system fits to a 1:1 binding model with an association constant of (8.1 ± 2.0) ×

dx.doi.org/10.1021/jp511351w | J. Phys. Chem. B XXXX, XXX, XXX−XXX

10^4 M^{-1}, in good agreement with the value obtained from the absorption experiments. This binding constant is more than 100 larger than that reported for β-cyclodextrin (590 M^{-1}) and is in line with increased evidence for the important contribution of hydrophobic effects to the binding free energy in cucurbituril complexes.[28,29] It is worth noting that in order to carry out the pH titration described below the addition of Na^+ cations to the system (as NaOH) cannot be avoided. Therefore, and in spite of the known competitive binding effects of this species with CB7, the association constant with β-naphthol was also determined in the presence of NaCl 10 mM (K_{ass} = (9.4 ± 1.0) × 10^3 M^{-1}).[30,31]

Figure 3 reports the pH-dependent β-naphthol absorption spectra and normalized fluorescence emission in the absence[13] and presence of cucurbit[7]uril. In the presence of 1 mM CB7, an apparent pK_a = 10.9 can be obtained from the pH titration experiments followed by UV−vis absorption spectroscopy. This value compares with that obtained in the absence of CB7 (pK_a = 9.5).[13] The increment observed in the pK_a values in the presence of CB7 suggests, as expected, that the neutral form of the β-naphthol displays higher affinity for forming inclusion complexes with CB7 in comparison with the ionized anionic form.[32] From the pK_a shift (ΔpK_a ≈ 1.4) a value of ≈370 M^{-1} can be estimated for the association constant of the phenolate with CB7 (in the presence of 10 mM NaCl). Guests included within the cavity of cucurbituril hosts usually display upward pK_a shifts. This behavior reflects the comparatively higher stabilization of positively charged or neutral acid forms to the respective neutral or anionic basic species. The values frequently observed for ΔpK_a range from below 1 up to 4, but the guest structural features that determine the magnitude of the ΔpK_a are not completely understood.[32]

The fluorimetric pH titration of β-naphthol in the absence of CB7 shows two inflection points: one at pH = 9.5 assigned to the pK_a of the ground state, and the second one at pH 2.4 attributed to the pK_{ap}^* of the excited state. Between pH ≈ 8 and ≈ 4, the acidic forms predominate in the ground state, but upon excitation emission from the acidic and basic species is observed because of ESPT. As anticipated by the emission spectra of β-naphthol in the presence of increasing concentrations of CB7 at pH 6.0 ± 0.2 (Figure 2b), the formation of the inclusion complex suppress the emission from the basic species. This can be due to effective suppression of the ESPT or to a shift of pK_{ap}^* to higher values.

In the presence of 0.125 mM CB7 (ca. 50% of β-naphthol is included in the CB7 cavity; see inset in Figure 3b), the pK_a increases to 10.2 but the pK_{ap}^* was found to be similar to that obtained in the absence of CB7 (pK_{ap}^* = 2.4). In addition, the η_{A^*} value decreases from 0.36 to 0.21. These observations indicate that the ESPT efficiency decreases as the result of a reduced fraction of free β-naphthol in solution. When virtually all β-naphthol is complexed (Figure 3c), no excited-state proton transfer is observed and the fluorescence and absorption titration curves are coincident (the obtained pK_a = 11.0 is in good agreement with that obtained from absorption spectroscopy). In practical terms, this means that no ESPT of β-naphthol takes place inside cucurbit[7]uril. Complete or partial inhibition of the ESPT by CB7 inclusion complexation has been previously reported for other guest molecules.[33−35] In these previous cases, the pK_{ap}^* is displaced to values higher than those observed in the absence of CB7, while in the present work the ESPT seems to be effectively suppressed. This contrasts with 4-methyl-7-hydroxyflavylium where ESPT is not precluded when the inclusion complex is formed, as will be shown below.

Flavylium Network of Chemical Reactions. Scheme 2 presents the chemical structure of flavylium cation. According to the nature and position of the substituents, several natural and synthetic flavylium derivatives have been described in the literature, comprising anthocyanins, the colorants responsible for most of the red and blue colors of flowers and fruits. In the case of anthocyanins, hydroxy substituents in position 7 and 4′ as well as a sugar either in position 3 (monoglucosides) or in position 3 and 5 (diglucosides) are necessary requirements. Position 3′ and 5′ can also bear hydroxy and methoxy substituents, defining the six more common anthocyanins. However, the flavylium cation is stable only in a restricted pH range (in anthocyanins, pH ≤ 1).

Scheme 2. Flavylium Cation

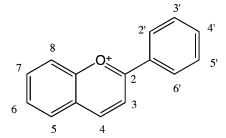

2-phenyl-1-benzopyrilium(flavylium)

The species shown in Scheme 3 can be reversible interconnected by external stimuli, such as pH, light, and temperature.

To simplify the system, the compound 4-methyl-7-hydroxyflavylium was selected. This is an exception of the flavylium family behavior, because in water only the proton-transfer equilibrium involving flavylium cation (AH^+) and quinoidal base (A) takes place.

ESPT of 4-Methyl-7-hydroxyflavylium. As mentioned above, the compound 4-methyl-7-hydroxyflavylium is an exception to the general flavylium network of chemical reactions because in water only the acid−base proton transfer takes place, with pK_a = 4.4.[12]

The fluorescence emission titration curves of the acidic and basic species are reported in Figure 4. Fitting with eqs 1 and 2 was achieved for pK_{ap}^* = −1 ± 0.3 and η_{A^*} = 0.93 ± 0.02.

The transient spectroscopy of this compound was studied in great detail by Maçanita and co-workers.[14−16] These authors found a value of 128 ps for the lifetime of the flavylium cation, 132 ps for the lifetime of the quinoidal base,[36] and more recently k_a^* = 2.5 × 10^{11} s^{-1} and k_{-a}^* = 2.3 × 10^{10} M^{-1} s^{-1}.[37] Substitution of these values in eq 6 leads to pK_{ap}^* = −0.93, in excellent agreement with data taken from the steady-state fluorescence emission titration.

The value of η_{A^*} is a useful parameter to account for the efficiency of the photoacid. The compound 4-methyl-7-hydroxyflavylium is thus one of the best examples reported in literature, which compares with 0.69 and 0.36 for 1-naphthol and 2-naphtol, respectively.[12,13]

ESPT of 4-Methyl-7-hydroxyflavylium in the Presence of Cucurbit[7]uril. Figure 5a shows the absorption spectra of 4-methyl-7-hydroxyflavylium (MHF) in the presence of different concentrations of CB7 at pH 1. The intensity of the maximum (414 nm) observed in the absorption spectrum of MHF decreases upon gradual addition of CB7 at pH 1. The association constant, K_{ass} = (5.1 ± 0.5) × 10^5 M^{-1}, for the inclusion complex formed between CB7 and the flavylium cation can be therefore obtained from the changes observed in

dx.doi.org/10.1021/jp511351w | J. Phys. Chem. B XXXX, XXX, XXX−XXX

Scheme 3. Network of Chemical Reactions Involving 7,4′-Dihydroxyflavylium[a]

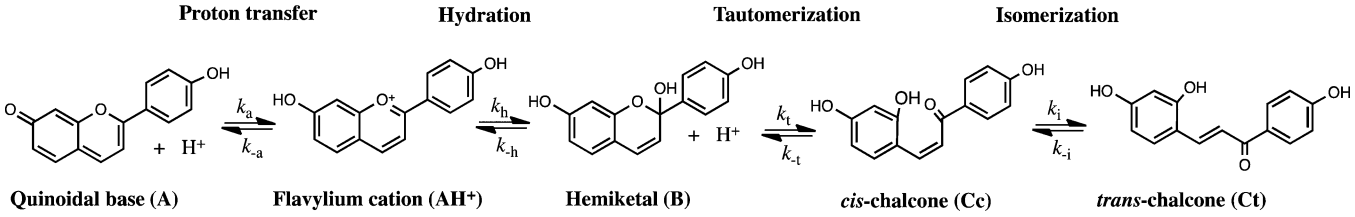

[a]Equilibrium constants defined as $K_n = k_n/k_{-n}$ (n = a, h, t, i).

Scheme 4. 4-Methyl-7-hydroxyflavylium

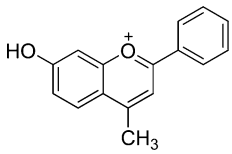

the absorption spectra (Figure 5a). On the other hand, the absorption spectrum of the quinoidal base (pH 9.2) does not change significantly upon addition of the host. Alternatively, the respective association constant can be readily obtained by fluorescence emission $(1.8 \pm 0.2) \times 10^4$ M^{-1}, Figure 5b. As in the case of the β-naphthol, the obtained association constant is higher for the acidic form of the guest, and the value obtained for the flavylium cation $(5.1 \pm 0.5) \times 10^5$ M^{-1} is similar to that previously observed for 3′,4′,7-trihydroxyflavylium (2.7×10^5 M^{-1}).[21] The magnitude of the ΔpK_a at infinite CB7 concentration can be estimated from the relation $\Delta pK_a = -\log_{10}(1.8 \times 10^4/5.1 \times 10^5) = 1.45$ and this value leads to $pK_a = 5.85$ for the inclusion complex.

Figure 6a shows the pH titration absorption spectra for MHF in the presence of 0.3 mM CB7. Under these conditions, a pK_a value of 5.6 ± 0.1 was obtained, which compares with 5.85 estimated from the association constants. This difference can be accounted for by the fact that in the presence of 0.3 mM the base is not fully complexed (ca. 84%) and the apparent pK_a obtained experimentally is expected to further increase with the CB7 concentration.

The pH titration curves of 4-methyl-7-hydroxyflavylium in the presence of CB7 0.3 mM obtained from fluorescence emission are shown in Figure 6. Contrary to what is observed for β-naphthol, the shape of the curves are similar to that obtained in the absence of host. However, some details deserve comment. While at 0.3 mM CB7 the acidic form is practically all inside the CB7, the base is only 84% complexed. Consequently, the contribution for the base emission from the acidic form upon the proton transfer in the excited state comes all from the AH^+@CB7. Conversely, the emission from direct excitation of the basic species, taking place at higher pH values, has two components: (i) one from the direct excitation of the base inside the CB7 and (ii) a minor component from the base in bulk water. The direct excitation of the quinoidal base in water occurs at lower pH values; thus, the titration curve acquires the shape reported in the figure. The obtained ground- and excited-state parameters are shown in Table 1 along with those obtained for β-naphtol. As can be observed, the ESPT of the compound 4-methyl-7-hydroxyflavylium seems not to be very much affected by its incorporation in CB7. This behavior strongly contrasts with that observed for β-naphtol and is probably related with the different structure of the host–guest complexes, as we try to shown below.

ESPT as Tool to Calculate the Ground-State Rate Constants k_a and k_{-a} of the Pair Flavylium/Quinoidal Base. Light absorption by flavylium compounds leads to a very efficient excited-state deprotonation, as discussed above. While deprotonation takes place in the excited state, proton recombination occurs in the ground state. Conversely, the quinoidal base can be formed by perturbing the system with pulsed radiation, and the kinetics of the proton recombination can be followed by transient-absorption spectroscopy with nanosecond resolution.[38]

As shown in Figure 7b, the second-order rate constants, corresponding to the reprotonation process, are the same within experimental error in the absence and presence of CB7 and equal to 2.7×10^{10} M^{-1} s^{-1}. This result is in good agreement with previous work in the absence of CB7.[36] The deprotonation constant is immediately obtained from the pH

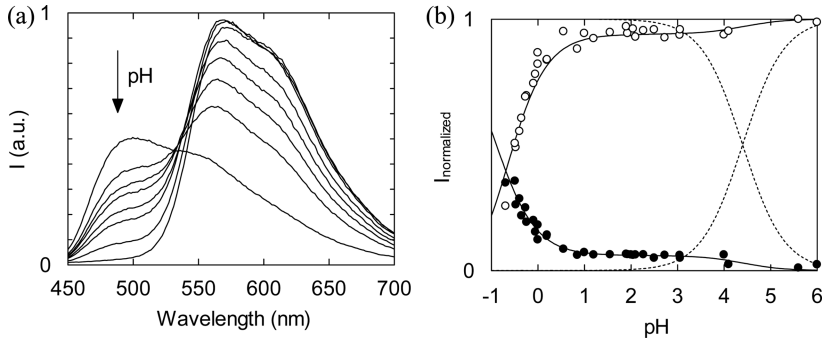

Figure 4. (a) Fluorescence emission spectra of the compound 4-methyl-7-hydroxyflavylium at the excitation wavelength 438 nm (isosbestic point). The pH was varied between 6 and −0.69. (b) Normalized fluorescence emission curves: (●) emission from the acidic species (λ_{em} = 493 nm); (○) emission from the basic species (λ_{em} = 603 nm); fitting achieved for $pK_a = 4.4$, $pK_{ap}^* = -1 \pm 0.3$, and $\eta_{A^*} = 0.93 \pm 0.02$, full lines; dashed lines show the mole fraction distribution of the ground state. Reproduced with permission from ref 22. Copyright 1998 Royal Society of Chemistry.

dx.doi.org/10.1021/jp511351w | J. Phys. Chem. B XXXX, XXX, XXX–XXX

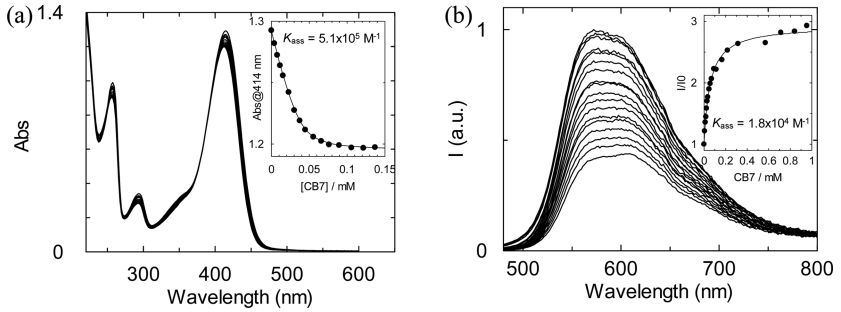

Figure 5. (a) Titration of the compound [MHF] 3.6×10^{-5} M at pH 1 followed by the absorption spectroscopy; (b) the same ([MHF] = 4.3×10^{-6} M) at pH 9.2 followed by fluorescence emission λ_{exc} = 460 nm and λ_{em} = 572 nm.

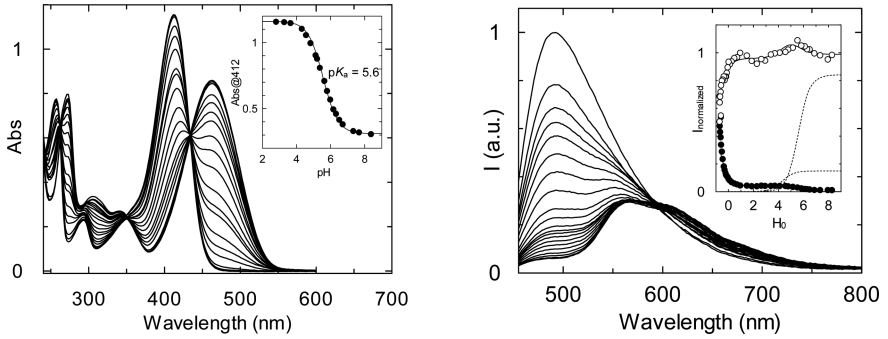

Figure 6. Titration curve of the compound 4-methyl-7-hydroxyflavylium (4.3×10^{-3} mM) in the presence of CB7 0.3 mM. Excitation at the isosbestic point (435 nm). (●) Emission from the acidic species (λ_{em} = 448 nm); (○) emission from the basic species (λ_{em} = 675 nm); fitting achieved for pK^*_{ap} = −1.1 ± 0.3 and η_{A^*} = 0.96 ± 0.02, full lines. The emission from the base has two components, from bulk A and A@CB7. The dashed lines represent the variation on the molar fraction distribution of A and A@CB7 with the pH.

Table 1. Parameters for Proton Transfer in the Excited State

compound	pK^*_{ap}	η_{A^*} (s^{-1})	pK_a
β-naphthol	2.4 ± 0.1	0.36 ± 0.01	9.5
β-naphthol@CB7	–	0	11.0
4-Me-7OH	−1 ± 0.3	0.93 ± 0.02	4.4
4-Me-7OH@CB7	−1.1 ± 0.3	0.96 ± 0.02	5.6

Table 2. Rate Constants for Proton Transfer in the Ground State

compound	pK_a	k_a (s^{-1})	k_{-a} ($M^{-1}\,s^{-1}$)
4-Me-7OH	4.3	1.3×10^6	2.7×10^{10}
4-Me-7OH@CB7	5.6	7.3×10^4	2.7×10^{10}

titration in the ground state, pK_a = 4.3 and 5.6 in the absence and presence of CB7, respectively (Table 2).

According to the data reported in Table 2, the host cucurbit[7]uril decreases the rate constant of the ground-state proton transfer more than 1 order of magnitude, stabilizing in this way the acidic form. It is interesting to stress that

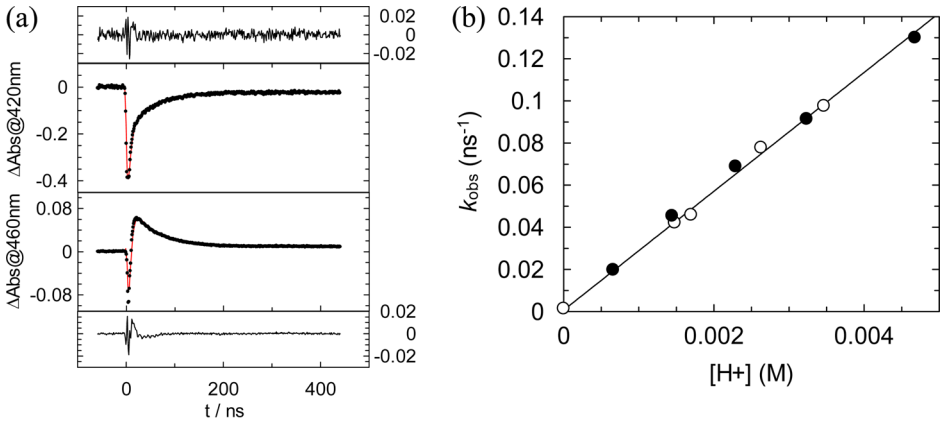

Figure 7. (a) Flash photolysis traces at 420 and 460 nm obtained upon laser excitation (λ_{exc} = 355 nm) of a MHF solution with CB7 0.8 mM at pH 3. The red lines correspond to the global fit taking into account the instrument response function, fluorescence, and the transient absorption of the ground-state back proton-transfer (see Experimental Section for details). (b) Rate constants of the flavylium absorption recover followed by flash photolysis upon laser excitation at λ_{exc} = 355 nm of the compound 4-methyl-7-hydroxyflavylium 0.05 mM in absence and presence of CB7: (○) in the absence of CB7; (●) in the presence of CB7 0.8 mM.

dx.doi.org/10.1021/jp511351w | J. Phys. Chem. B XXXX, XXX, XXX−XXX

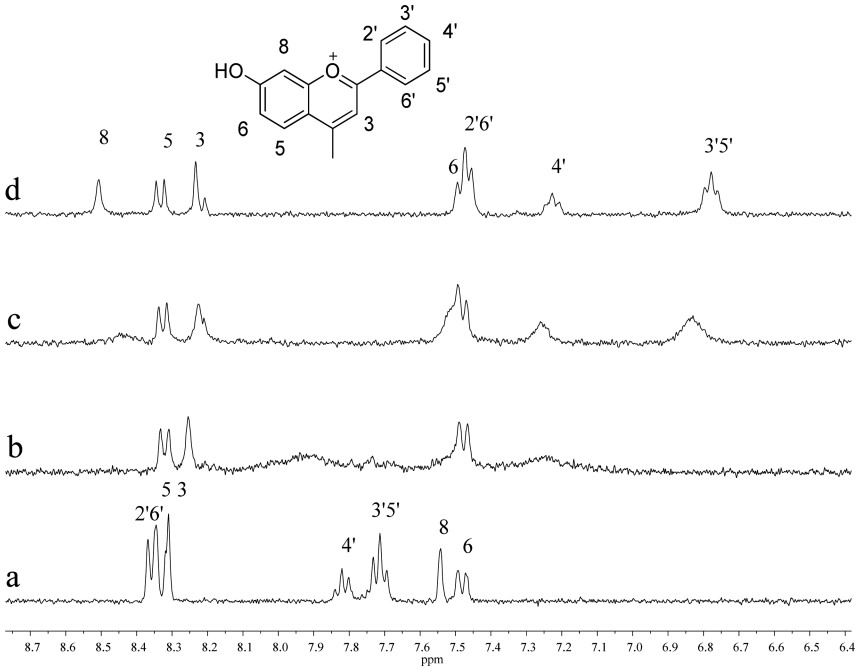

Figure 8. Partial ^{1}H NMR spectra of 4-methyl-7-hydroxyflavylium (0.5 mM) in D_2O pD = 1 with increasing concentrations of CB7: (a) 0 equiv, (b) 0.5 equiv, (c) 1 equiv, and (d) 2 equiv.

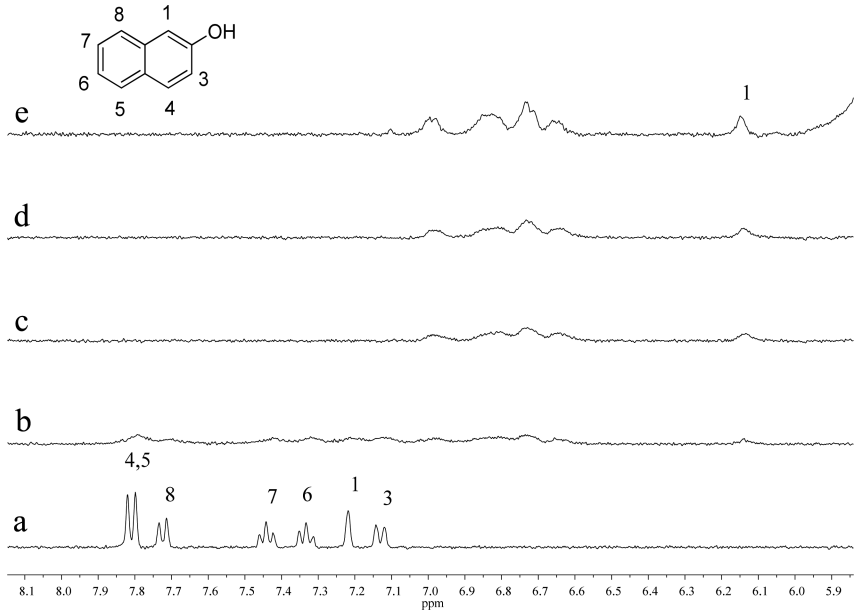

Figure 9. Partial ^{1}H NMR spectra of β-naphthol (0.5 mM) in D_2O with increasing concentrations of CB7: (a) 0 equiv, (b) 0.5 equiv, (c) 1 equiv, (d) 1.5 equiv, and (e) 4.7 equiv.

protonation of the base is controlled by the diffusion and is not affected by the host.

^{1}H NMR Experiments. The data regarding the ^{1}H NMR spectra of the adducts of β-naphthol and 4-methyl-7-hydroxyflavylium with the host cucurbit[7]uril (CB7) are reported in Figures 8 and 9. The differences observed in the spectra of the free and complexed species provide valuable information concerning the structures of the complexes. It is accepted that the signals of the guest protons located near the carbonyl portals of the host are displaced downfield while the signals corresponding to the protons included inside the cavity are displaced upfield.[39] As can be observed in Figure 8, the ^{1}H NMR signals corresponding to the phenyl group of 4-methyl-7-hydroxyflavylium are displaced upfield ($\Delta\delta(4') = -0.593$ ppm, $\Delta\delta(3',5') = -0.926$ ppm, and $\Delta\delta(2',6') = -0.882$ ppm), suggesting that this group is included inside the cavity of CB7 while the signals corresponding to the protons of the benzopyrylium group are affected to a lesser extent. Protons 5 and 6 are pratically unaffected, while proton 3 is slightly displaced upfield (−0.09 ppm) and proton 8 displaced downfield (0.965 ppm). This set of observations suggests that CB7 selectively include the phenyl moiety of 4-methyl-7-hydroxyflavylium while the benzopyrylium remains (partially) outside the cavity. The high downfield displacement observed

dx.doi.org/10.1021/jp511351w | J. Phys. Chem. B XXXX, XXX, XXX−XXX

for proton 8 suggests that the carbonyl oxygen of CB7 might establish hydrogen bonds with that proton. This binding mode contrasts with that observed for 3′,4′,7-trihydroxyflavylium. In this case it was observed that CB7 shuttles rapidly between the phenyl and the benzopyrylium rings.[21]

The same type of ^{1}H NMR experiment was also carried out for β-naphthol guest. In this case, the ^{1}H NMR signals of the complex partially overlap, precluding the signals from being unequivocally attributed. However, it is clear that all ^{1}H NMR signals of β-naphthol are displaced upfield upon inclusion in the cavity of CB7 (see Figure 9). This suggests that the molecule is deeply included inside the cavity of the host. Figure 10 shows

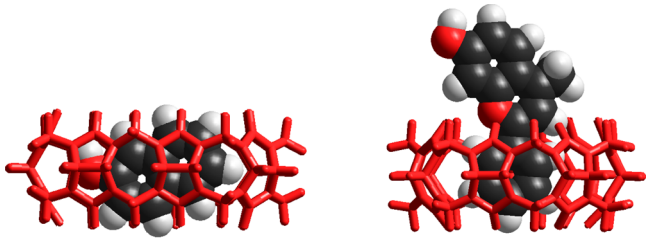

Figure 10. Representation of the possible structures for the adducts of β-naphthol and 4-methyl-7-hydroxyflavylium with cucurbit[7]uril.

some possible structures of the inclusion complexes proposed on the basis of the ^{1}H NMR experiments. However, other structures with the naphthyl group included in the cavity and the hydroxyl group localized near the carbonyl portal are also possible. In this case, hydroxyl group is able to establish hydrogen bond with the carbonyl oxygens of the host. Nevertheless, it is clear that while the ionizable OH group of β-naphthol can be kept away from contact with the solvent, by complete inclusion or by hydrogen bonding with the host, in the case of the flavylium derivative the ionizable OH is far from the cavity of the host.

The proposed structures can explain why the ESPT of β-naphthol is completely precluded by the complexation with CB7 whereas for the flavylium guest the ESPT is not affected. This is also in good agreement with the observation that the ground-state protonation rate constant of the flavylium compound is not affect by the formation of the inclusion complex (Figure 7). Unfortunately, the same type of experiment cannot be performed with β-naphthol because the ESPT is completely suppressed.

Previous work by Köhler and co-workers supports the proposed hypothesis. The authors observed that ESPT of β-naphthol is effectively suppressed when 2:1 host−guest complexes are formed with α-cyclodextrin but only partially in the case of 1:1 complexes with α- and β-cyclodextrin.[28]

CONCLUSIONS

Steady-state fluorescence emission titration curves while not giving mechanistic details of the ESPT processes are still a very useful tool to account for this phenomenon. Crucial information can be achieved upon interpretation of the data through a mathematical model recast from the Weller theory. Of particular significance is the parameter η_{A^*}, which measures the efficiency of the photoacid. The ESPT is very dependent on the chemical environment because a molecule (or a molecular moiety in the case of intramolecular ESPT) functioning as proton acceptor is necessary. By taking two molecules frequently employed in ESPT studies, β-naphthol and 4-methyl-7-hydroxyflavylium, it was demonstrated in the present work that the ESPT is highly dependent on structure of the host−guest complex and that no ESPT takes place when the phenol is completely surrounded by the cucurbit[7]uril cavity. Therefore, it seems to depend more on the orientation of the guest molecule inside the host's cavity than on the relative stabilization of the basic and acid forms. This result contrasts with the acid−base chemistry of host−guest complexes on the ground state than can be easily predicted from the relative affinity of the host for the acid and basic forms of the guest.

AUTHOR INFORMATION

Corresponding Authors

*E-mail: nuno.basilio@fct.unl.pt.
*E-mail: fp@fct.unl.pt.

Notes

The authors declare no competing financial interest.

ACKNOWLEDGMENTS

This work was supported by the European project NMP4-SL-2012-310651 under FP7-NMP-2012-SMALL-6 and Fundação para a Ciência e Tecnologia, Project PTDC/QUI-QUI/117996/2010. N.B. acknowledges a postdoctoral grant, SFRH/BPD/84805/2012. The NMR spectrometers are part of The National NMR Facility, supported by Fundação para a Ciência e a Tecnologia (RECI/BBB-BQB/0230/2012).

REFERENCES

(1) Crespo, H.; Cohen, B.; Hare, P. M.; Koheler, B. Ultrafast Excited-State Dynamics in Nucleic Acids. *Chem. Rev. (Washington, DC, U.S.)* **2004**, *104*, 1977−2019.
(2) Agmon, A. Elementary Steps in Excited-State Proton Transfer. *J. Phys. Chem. A* **2005**, *109*, 13−35.
(3) Tolbert, L. M.; Solntsev, K. M. Excited-State Proton Transfer: From Constrained Systems to "Super" Photoacids to Superfast Proton Transfer. *Acc. Chem. Res.* **2002**, *35*, 19−27.
(4) Douhal, A. Ultrafast Guest Dynamics in Cyclodextrins Nanocavities. *Chem. Rev. (Washington, DC, U.S.)* **2004**, *104*, 1955−1976.
(5) Arnaut, L. G.; Formosinho, S. J. Excited-State Proton-Transfer Reactions. 1. Fundamentals and Intermolecular Reactions. *J. Photochem. Photobiol., A* **1993**, *75*, 1−20.
(6) Shizuka, H. Excited-State Proton Transfer Reactions and Proton-Induced Quenching of Aromatic Compounds. *Acc. Chem. Res.* **1985**, *18*, 141−147.
(7) Robinson, G. W. Proton Charge Transfer Involving the Water Solvent. *J. Phys. Chem.* **1991**, *95*, 10386−10391.
(8) Weller, A. Quantitative Untersuchungen der Fluoreszenzunwandlung bei Naphtholen. *Z. Elektrochem.* **1952**, *56*, 662−686.
(9) Weller, A. Allgemeine Basenkatalyse bei der Elektrolytischen Dissoziation Angeregter Naphthole. *Z. Elektrochem.* **1954**, *58*, 849−853.
(10) Harris, B. K.; Selinger, K. Photo Induced Fluorescence Quenching of 2-Naphthol. *J. Phys. Chem.* **1980**, *84*, 891−898.
(11) Harris, B. K.; Selinger, K. Acid−Base Properties of 1-Naphthol. Proton-Induced Fluorescence Quenching. *J. Phys. Chem.* **1980**, *84*, 1366−1371.
(12) Melo, M. J.; Bernardo, M. A.; Melo, E.; Pina, F. Shape of Acid−Base Fluorescence Emission Titration Curves in the Presence of Buffer and Quenching Effects. *J. Chem. Soc. Faraday Trans.* **1996**, *92*, 957−968.
(13) Melo, M. J.; Melo, E.; Pina, F. Determination of Acid-Base Equilibria of Organic Pollutants: The Steady State Fluorescence Emission Method. *Arch. Environ. Contam. Toxicol.* **1994**, *26*, 510−520.
(14) Freitas, A. A.; Maçanita, A. L.; Quina, F. H. Improved Analysis of Excited State Proton Transfer Kinetics by the Combination of

Standard and Convolution Methods. *Photochem. Photobiol. Sci.* **2013**, *12*, 902−910.
(15) Giestas, L.; Yihwa, C.; Lima, J. C.; Vautier-Giongo, C.; Lopes, A.; Maçanita, A. L.; Quina, F. H. The Dynamics of Ultrafast Excited State Proton Transfer in Anionic Micelles. *J. Phys. Chem. A* **2003**, *107*, 3263−3269.
(16) Rodrigues, R.; Vautier-Giongo, C.; Silva, P. F.; Fernandes, A. C.; Cruz, R.; Maçanita, A. L.; Quina, F. H. Geminate Proton Recombination at the Surface of SDS and CTAC Micelles Probed with a Micelle-Anchored Anthocyanin. *Langmuir* **2006**, *22*, 933−940.
(17) Rebek, J. Molecular Behavior in Small Spaces. *Acc. Chem. Res.* **2009**, *42*, 1660−1668.
(18) Lee, J. W.; Samal, S.; Selvapalam, N.; Kim, H.-J.; Kim, K. Cucurbituril Homologues and Derivatives: New Opportunities in Supramolecular Chemistry. *Acc. Chem. Res.* **2003**, *36*, 621−630.
(19) Isaacs, L. Stimuli Responsive Systems Constructed Using Cucurbit[*n*]uril-Type Molecular Containers. *Acc. Chem. Res.* **2014**, *47*, 2052−2062.
(20) Kaifer, A. E. Toward Reversible Control of Cucurbit[*n*]uril Complexes. *Acc. Chem. Res.* **2014**, *47*, 2160−2167.
(21) Basílio, N.; Pina, F. Flavylium Network of Chemical Reactions in Confined Media: Modulation of 3′,4′,7-Trihydroxyflavilium Reactions by Host−Guest Interactions with Cucurbit[7]uril. *ChemPhysChem* **2014**, *15*, 2295−2302.
(22) Pina, F.; Melo, M. J.; Santos, H.; Lima, J. C.; Abreu, I.; Ballardini, R.; Maestri, M. Excited State Proton Transfer in Synthetic Flavylium Salts: 4-Methyl-7-Hydroxyflavylium and 4′,7-Dihydroxyflavylium. *New J. Chem.* **1998**, *22*, 1093−1098.
(23) Pina, F.; Melo, M. J.; Alves, S.; Ballardini, R.; Maestri, M.; Passaniti, P. Micelle Effect on Ground and Excited State Proton Transfer Reactions Involving the 4-Methyl-7-Hydroxyflavylium Cation. *New J. Chem.* **2001**, *25*, 747−752.
(24) Basilio, N.; García-Río, L.; Moreira, J. A.; Pessêgo, M. Supramolecular Catalysis by Cucurbit[7]uril and Cyclodextrins: Similarity and Differences. *J. Org. Chem.* **2010**, *75*, 848−855.
(25) Yi, S.; Kaifer, A. E. Determination of the Purity of Cucurbit[*n*]uril (*n* = 7, 8) Host Samples. *J. Org. Chem.* **2011**, *76*, 10275−10278.
(26) Snellenburg, J. J.; Laptenok, S. P.; Seger, R.; Mullen, K. M.; van Stokkum, I. H. M. Glotaran: A Java-Based Graphical User Interface for the R Package TIMP. *J. Statistical Software* **2012**, *49*, 1−22.
(27) Bell, R. P. *The Proton in Chemistry*; Chapman and Hall: London, 1973.
(28) Park, H.; Mayer, B.; Wolschann, P.; Köhler, G. Excited-State Proton Transfer of 2-Naphthol Inclusion Complexes with Cyclodextrins. *J. Phys. Chem.* **1994**, *98*, 6158−6166.
(29) Biedermann, F.; Nau, W. M.; Schneider, H.-J. The Hydrophobic Effect Revisited—Studies with Supramolecular Complexes Imply High-Energy Water as a Noncovalent Driving Force. *Angew. Chem., Int. Ed.* **2014**, *53*, 11158−11171.
(30) Ong, W.; Kaifer, A. E. Salt Effects on the Apparent Stability of the Cucurbit[7]uril − Methyl Viologen Inclusion Complex Inclusion Complex. *J. Org. Chem.* **2004**, *69*, 1383−1385.
(31) Tang, H.; Fuentealba, D.; Ko, Y. H.; Selvapalam, N.; Kim, K.; Bohne, C. Guest Binding Dynamics with Cucurbit[7]uril in the Presence of Cations. *J. Am. Chem. Soc.* **2011**, *133*, 20623−20633.
(32) Ghosh, I.; Nau, W. M. The Strategic Use of Supramolecular pK_a Shifts to Enhance the Bioavailability of Drugs. *Adv. Drug Delivery Rev.* **2012**, *64*, 764−783.
(33) Wang, R.; Yuan, L.; Macartney, D. H. A Green to Blue Fluorescence Switch of Protonated 2-Aminoanthracene upon Inclusion in cucurbit[7]uril. *Chem. Commun. (Cambridge, U.K.)* **2005**, 5867−5869.
(34) Shaikh, M.; Dutta Choudhury, S.; Mohanty, J.; Bhasikuttan, A. C.; Nau, W. M.; Pal, H. Modulation of Excited-State Proton Transfer of 2-(2′-Hydroxyphenyl)benzimidazole in a Macrocyclic Cucurbit[7]uril Host Cavity: Dual Emission Behavior and pK_a Shift. *Chem.—Eur. J.* **2009**, *15*, 12362−12370.
(35) Gavvala, K.; Sengupta, A.; Koninti, R. K.; Hazra, P. Supramolecular Host-Inhibited Excited-State Proton Transfer and Fluorescence Switching of the Anti-Cancer Drug, Topotecan. *ChemPhysChem* **2013**, 3375−3383.
(36) Lima, J. C.; Abreu, I.; Brouillard, R.; Maçanita, A. L. Kinetics of Ultra-fast Excited State Proton Transfer from 7-Hydroxy-4-methylflavylium Chloride to Water. *Chem. Phys. Lett.* **1998**, *298*, 189−195.
(37) Freitas, A. A.; Quina, F. H.; Maçanita, A. L. Picosecond Dynamics of Proton Transfer of a 7-Hydroxyflavylium Salt in Aqueous−Organic Solvent Mixtures. *J. Phys. Chem. A* **2011**, *115*, 10988−10995.
(38) Maçanita, A. L.; Moreira, P. F.; Lima, J. C.; Quina, F. H.; Yihwa, C.; Vautier-Giongo, C. Proton Transfer in Anthocyanins and Related Flavylium Salts. Determination of Ground-State Rate Constants with Nanosecond Laser Flash Photolysis. *J. Phys. Chem. A* **2002**, *106*, 1248−1255.
(39) Pessêgo, M.; Moreira, J. A.; Rosa da Costa, A. M.; Corrochano, P.; Poblete, F. J.; Garcia-Rio, L. Electrostatic Repulsion Between Cucurbit[7]urils Can Be Overcome in [3]Pseudorotaxane without Adding Salts. *J. Org. Chem.* **2013**, *78*, 3886−3894.